Modeling of Output Spectra and Numerical Simulation of Thulium-doped Broadband Fiber Light Sources at 1400-1520nm, 1800-2000nm

Zhaojun Sun*

School of Avionics and Electricity, Civil Aviation Flight University of China, Sichuan, China

* Corresponding Author Email: 1201003027@cnu. edu. cn

Abstract. Lasers have a great influence in industrial processing and biomedical fields. Thulium-doped fiber lasers have good prospects for communication transmission and polymer welding. In this paper, the research method is as follows: in the pump light at 0. 79um, the values of Thulium-doped fiber, including its core radius, spontaneous radiation rate, cross-sectional absorption area, etc., are preset in advance. Then, by changing the fiber length, pumping power, and doping concentration of the fiber, the curve between the output spectrum of ASE light and the wavelength of ASE light is demonstrated. Finally, the peak power of the Thulium-doped broadband light source fiber is about 1. 6×10^{-9}w at L=3m, N=4×$10^{24}/m^3$, Pp=0. 2w. The output spectrum of thulium-doped fiber is mainly concentrated around the 2000nm wavelength band, and examples of thulium-doped fiber lasers for modern medical and industrial fields are presented. The thulium-doped fiber is the main direction of future research and the outlook for the future.

Keywords: Laser; Thulium-Doped Fiber; Output Spectrum; ASE Optical Power.

1. Introduction

Historically, society has been quite concerned about 2μm Thulium-doped fiber lasers. Whether it is Xiaoxi Jin, in the research for high-power Thulium-doped fiber, designed a very stable superb fluorescent light source and finally obtained a higher than 300W output power laser [1]. 2015, double cladding Thulium-doped fiber in the research [2], but the cladding absorption and slope efficiency do not reach very high values, so Thulium-doped fiber is the more cutting-edge development in the future. Still using the 2μm band containing 2μm, 1. 8μm, 1. 9μm, and other wavelength ranges previously studied, Central South University for Nationalities [3] in 2015 conducted a study on the spectral absorption of water molecules and selected the absorption spectrum at 1. 1-1. 7μm. eventually, the measurement of water by absorption spectroscopy can be achieved. In addition, there are presentations in the fields of laser medicine and laser weapons [4, 5]. The uses of lasers are very diverse and deserve to be further investigated.

Lasers play a major role in industry and can be useful in changing surface properties, finely processing materials, detection of objects technology [6], etc. In biomedicine, the Southwest Institute of Technology and Physics [7] has been used in different excitation wavelengths to correspond to different substances to determine their concentration size and avoid biological damage. In addition, the Guangdong General University Key Laboratory of Advanced Optical Precision Manufacturing Technology, Shenzhen University of Technology [8] used a Thulium-doped fiber laser with a central wavelength of 1939. 31, adjustable pulse width from 0 to 2000 μs, adjustable repetition frequency from 0 to 2 kHz, and maximum average output power of 34. 2 W. The pulse repetition frequency was increased to improve the lithotripsy rate and the energy to the size of the change ablation.

In the last five years, the Thulium-doped fiber laser is still the main direction of research, which has the advantages of light and compact structure, good beam stability, and good heat dissipation capability. It has been widely used in many fields, such as medical engineering, exploration operations, and transmission communication [9]. In 2017, Wang Xiaofa et al. [10] obtained a repetition frequency of 3. 8 MHz using a laser of nanosecond-locked mode Thulium-doped fiber with its toroidal and an output of 2μm nanosecond mode-locked pulses that can be varied arbitrarily in the range of 3. 8-9. 43ns. In general, Thulium-doped fibers are designed with cladding over the core. In

the same year, Tianjin University [11] used a double-cladding design and conducted a study on its temperature. They found that Thulium-doped fiber amplifiers are suitable for lower peak temperatures, with larger pump optical power and a Gaussian distribution function of the absorption cross-section. Four years ago, Zhang Wei et al. [12] let 793 nm, 142. 9 W pump light into the fiber on a high power narrow spectral width Thulium-doped fiber laser and obtained an average power of 90 W with a central wavelength of 1915 nm, slope efficiency of 60. 2%, light ray conversion of 63%, and excellent quality laser output. 2021, Xi'an Medical College [13] conducted an in-depth study on double-clad fiber. The results showed that the more reflections, the higher the pump absorption rate approaches 100%, and the shape of the cladding changes, and the new inner cladding has the highest absorption efficiency. Two shapes of cladding, ortho-hexagonal, and new inner cladding fiber lasers, were selected, and the output power of the new inner cladding fiber was 12. 1% higher than that of the ortho-hexagonal.

The Thulium-doped fiber laser used in this simulation can be varied in length, wavelength, and doping concentration to obtain peak power at different wavelengths. The energy level system of the Thulium element in this simulation is determined first. The velocity equation is expressed, and then the power equation is written. The ASE optical power varies with length, wavelength, and doping concentration. Finally, the desired parameters are found and brought into the equation to obtain the desired output spectrum. Finally, its conclusion is analyzed and presented.

2. Models and Methods

2.1. Thulium ion's three-energy structure

In the energy level of Thulium ion, there are many photon energy levels. In this simulation, a three-state energy level system is chosen: ground state energy level, excited state energy level, and sub-steady state energy level, which is a three-energy level system [14] (Fig. 1).

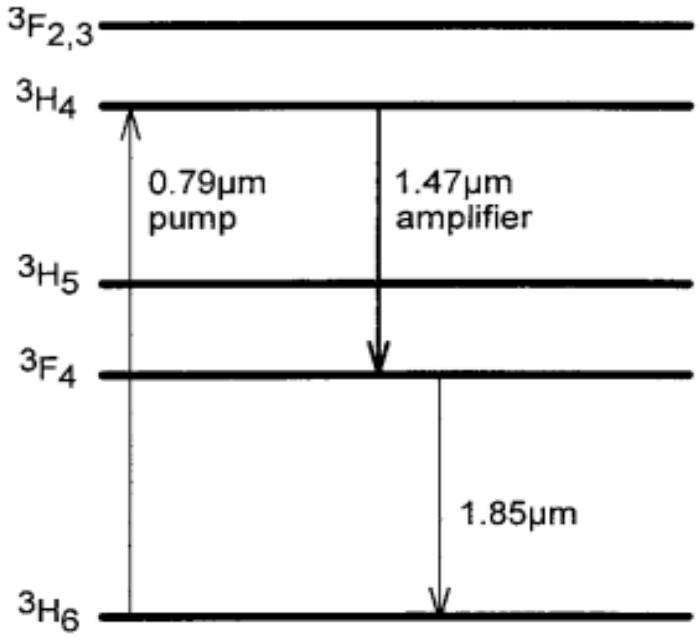

Fig 1. Energy-level diagram of Tm^{3+}[14].

The electron is in the stable ground state $^3H_6$ and will jump from the ground state to the excited state $^3H_4$ due to the irradiation of the 0. 79um pump light. However, the excited state is unstable, and the electron will jump from the excited state to the sub-stable state $^3F_4$ while generating 1. 47um of the signal light. The photons on the sub-stable state produce spontaneous radiation and jump from the sub-stable state to the ground state while emitting 1. 89um of ASE (Amplified spontaneous emission) light.

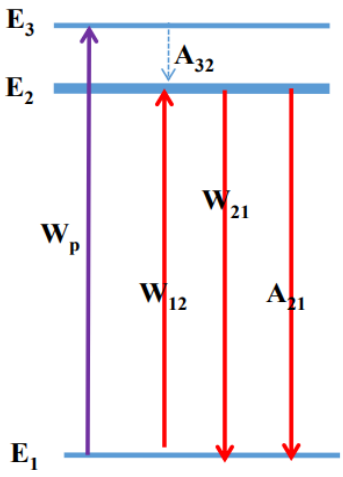

Fig 2. Three-energy energy level diagram.

Fig. 2 shows the three-energy level system, in which Wp is the pump light absorption rate, which is the absorption rate at which the pump light raises the electrons at the E_1 energy level to the E_3 energy level, i. e, E_1 toE_3. W_{12} Is the signal light absorption rate and W_{21} is the signal light stimulated emission rate. A_{32} Is the radiation-free leap rate from three energy levels to two energy levels? Its value indicates that although the electron leaps at the energy level, it does not radiate a photon, so it is a radiation-free leap. A_{21} is the radiated light produced by the spontaneous radiation from E_2 energy level to E_1 energy level, which is the ASE light introduced later in this paper. The first three rates can be represented in the simulation software in the form of expressions, i. e.Wp , W_{12} , W_{21}.

2.2. Writing of the rate equation

The numerator of Wp is the product of the pump light absorption cross-sectional area (σ_{13}) and the pump light power ($P_{p(z)}$, which varies with length), and the numerator is the frequency of the radiated electromagnetic wave (v_{13}) at the E_1 to E_3 energy levels multiplied by Planck's constant (h, and the product of the two is the energy of the electron), multiplied by$Aeff$. Where $Aeff$ can be calculated by$Aeff = \pi r^2$.

W_{12} Is also the same asWp, the calculation formula also requires the cross-sectional absorption area. The difference is that W_{12} requires the use of σ_{12} notσ_{13}, because it expresses the signal light absorption rate. v_{12} Also refers to E_1 to E_2 energy levels of the frequency of electromagnetic radiation waves.

2.3. Particle conservation

Because electrons are conserved, the number does not increase and decrease. Therefore, the number of electrons will change between the three levelsE_1,E_2, and E_3 because of the absorption and release of light. However, since the total number of electrons in the fiber is constant, the expressions for the change in the number of electrons seen in the three levels can be listed, and the sum of the three equations can be zero.

The column writes the change of the number of particles in the first energy level with time: because in$N_1(z)$, $W_p(z)$ and $W_{12}(z)$ will release electrons to E_3 andE_2, so here is the negative sign. At the same time, $N_1(z)$ will also receive the signal light radiated from the second energy level to the first energy level with the ASE light spontaneously radiated. These two items need to be added and preceded by a positive sign. The change of $N_2(z)$ with time is also the same, and the two electrons absorbed by E_1 to E_2 and released by E_3 to E_2 are positive, followed by subtracting the two electrons released to the E_1 energy level. $N_3(z)$ Is also the same, not here to repeat?

In a whole fiber, it is a whole, so it is necessary to add$N_1(z)$,$N_2(z)$, and $N_3(z)$ and make it zero, because the electrons are conserved.

The detailed expressions of N_1, N_2, N_3 can be finally obtained by solving the differential equations with constant coefficients in Matlab for the three and four formulas.

2.4. Establishment of the power qeuation

Establish the variation of P_p pump power and $P_{ase(z)}$ (ASE power with length), which essentially means that the electrons lost by the pump source at $N_1(z)$ are multiplied by the pump light emission interface σ_ρ, and then subtract the overall background loss a_a multiplied by the overlap factor Γ_p and $P_\rho(z)$, again a constant coefficient differential equation. The ASE optical power is similar to that by the pump frequency, $N_1(z)$ cross-section received by $N_2(z)$ released by the electrons, denoted by $\sigma_{21}N_2(z)$ in Eq. At the same time, $N_1(z)$ releases electrons to$N_2(z)$, denoted by $-\sigma_{12}N_1(z)$, while subtracting the corresponding background loss a_s. The overall multiplication of $P_{s(z)}$ and the ASE overlap factor Γase is also required. Add to this the energy of the photons released by$N_2(z)$ $\sigma_{21}N_2(z)h_{v\Delta_v}$. Δv is the frequency half height full width (Hz).

2.5. Enumeration of overlaping factors

The overlap factor has Γ_p and Γase in the power equation, respectively, both are calculated by the same formula. $\Gamma_\rho = 1 - e^{\left(-2\frac{r^2}{w^2}\right)}, w = r\left(0.65 + \frac{1.619}{v^{\frac{3}{2}}} + \frac{2.879}{v^6}\right), v = \frac{2\pi r}{\lambda}(n_1^2 - n_2^2)^{\frac{1}{2}}$. r and w are the fiber core radius and square mode field radius (unit: m), v is the normalized frequency of the fiber. n_1 And n_2 are the core refractive index and cladding refractive index, respectively, with values of n_1 = 1. 62 and n_2 = 1. 52.

3. Results and Discussion

The data in Table 1 are all the data used in this simulation.

Table 1. Simulation Data.

Category	Numerical value
Pump light wavelength (m)	7.9×10^{-7}
Fiber core radius(m)	2.5×10^{-5}
A21(s^{-1})	500[15]
A32(s^{-1})	300[15]
Sigma21(m^2)	The values of the fitted curves in the literature [16]
Sigma12(m^2)	The values of the fitted curves in the literature [16]
a(m^{-1})	0. 1
Sigma13(m^2)	8.9×10^{-26}
Doping concentration	4×10^{24}

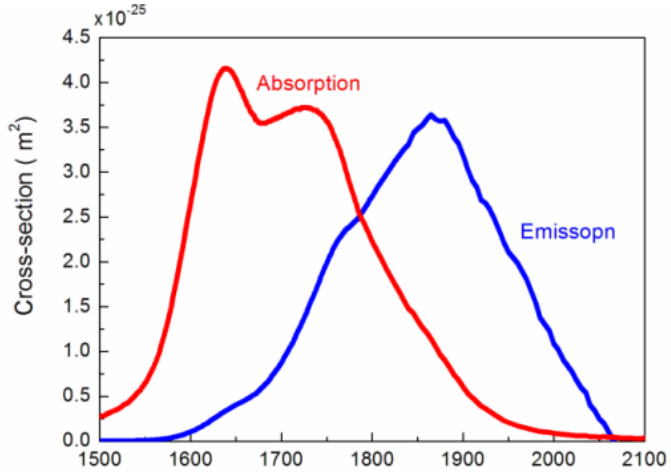

Fig 3. Absorption and emission curves.

Fig. 3 shows the relationship between the absorption and emission cross-sections used at different wavelengths this time. The Fig. does not list its absorption and emission cross section at 1400-1500 nm, so it is taken as 0. The ASE power is related to the length, doping concentration, and pumping power by solving the constant coefficient differential equation for the ASE optical frequency. I set the three variables at L=2m, 3m, 4m, N=2×10^{24}, 4×10^{24}, 6×10^{24}, Pp=0. 4w, 0. 6w, 0. 8w, respectively, to simulate them in Matlab and save the pictures.

The first variable is the fiber length, and the output spectra obtained by changing the fiber length to L=2m, 3m, and 4m, respectively, are shown in Fig. 4(a).

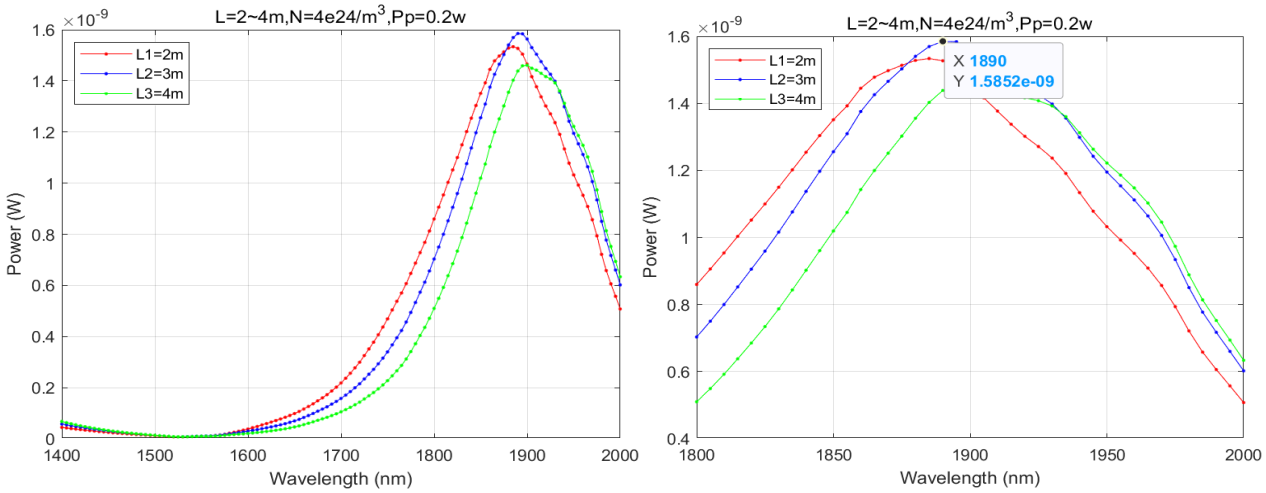

Fig 4. (a). Output spectrum obtained by varying the fiber length.
(b). 1800~2000nm magnification example.

Figure. 4(b) shows the enlarged example of Figure. 4(a) in the 1800-2000nm interval. By marking the points with the software, the output spectrum is found to peak at 1885nm with a wavelength of about 1. 53×10^{-9}w at L=2m, at 1890nm with a wavelength of about 1. 59×10^{-9}w at L=3m, and at L=4m. Because the output spectral band of the Thulium-doped fiber laser is mainly concentrated in 1700-2100nm, there are corresponding peaks in this range in the output spectrum simulation.

Under the three conditions, the position of the wavelength where the output power is located does not change much, with a maximum change of 10 nm and a minimum peak wavelength change of only 5 nm. The power values of the output spectrum are boosted by about 4% for 2m vs. 4m and about 4% for 3m vs. 2m. However, changing the fiber length is not the main variable that changes the power delivery.

The second variable is the fiber doping concentration, and three doping concentrations, N=2×10^{24}, 4×10^{24}, and6×10^{24}, were selected to model the data, and the results are shown in Fig. 5(a).

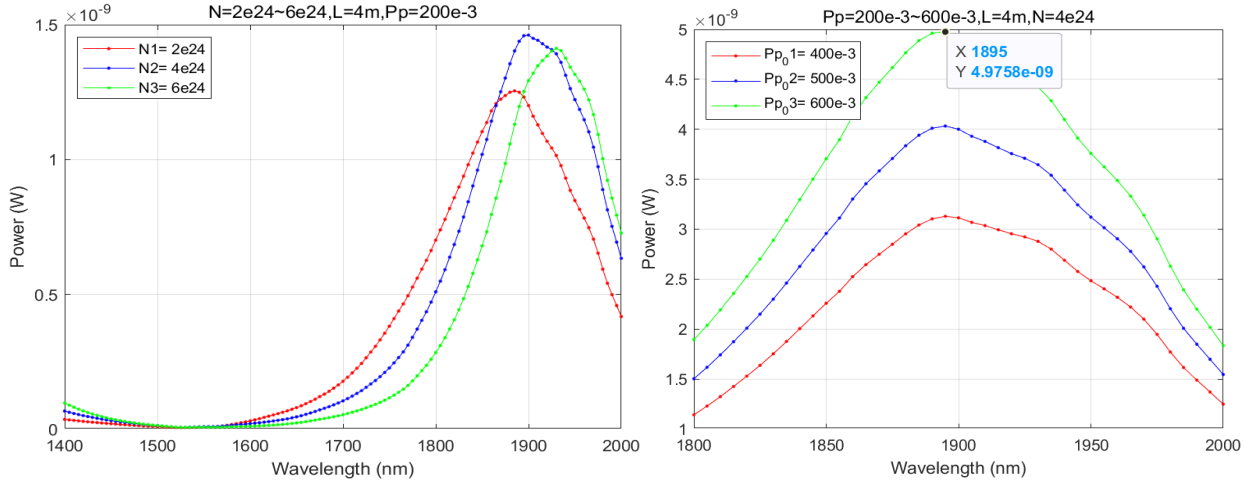

Fig 5. (a). Output spectra obtained by changing the doping concentration. (b). 1800~2000nm magnification example.

Three curves were fitted by varying the concentration, and the red curve is the output power of about 1. 25×10^{-9} at a wavelength of 1885 nm obtained at a concentration of 2×10^{24}. At a doping concentration of 4×10^{24}, there is the optimal output spectrum value of about 1. 46×10^{-9}.

The third variable is the pump optical power, and by setting Pp = 0. 4w, 0. 6w, and 0. 8w, the images of the output spectra are shown in Figure. 6 (a).

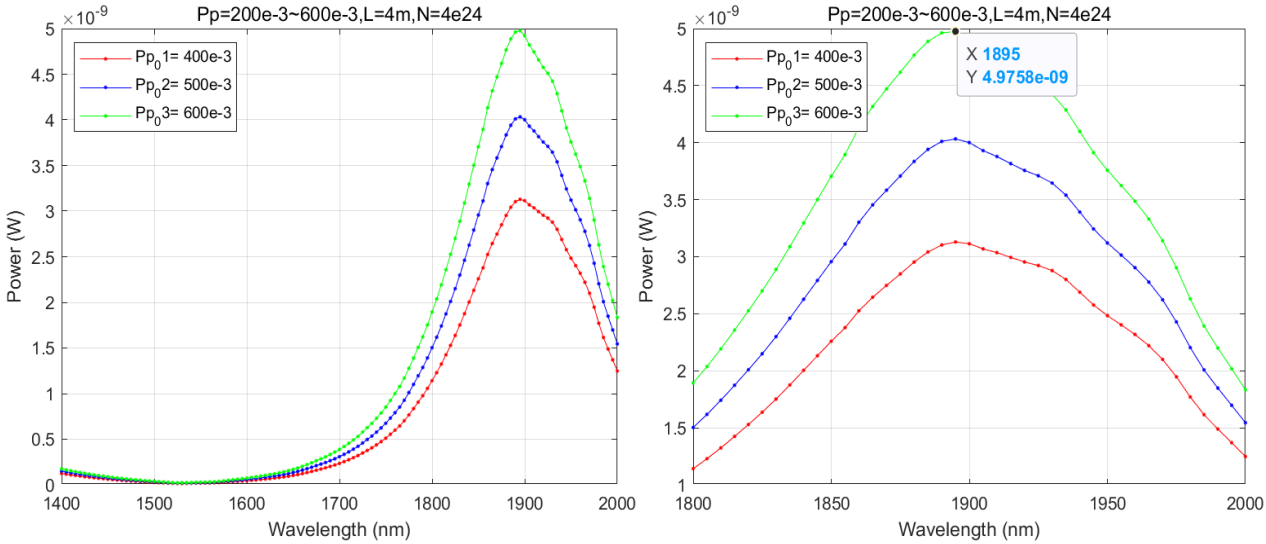

Fig 6. (a). Output spectrum obtained by changing the pump power
(b). 1800~2000nm magnification example.

After modeling, it is found that a new peak in ASE power occurs as the pump power increases. Fig. 6 shows an example of its magnification from 1800 nm to 2000 nm. After the pump power is 0. 4w and the wavelength is 1895nm, the peak is observed to be about 3. 13×10^{-9}w. After that, the pump power is adjusted to 0. 4w and 0. 6w, respectively. The output power of 0. 4w is increased by about 29% compared to 0. 2w. the output power of 0. 6w pump light is increased by about 24% compared to 0. 4w. Therefore, the pump light power is the key factor affecting the output spectrum. After that, the pump power was increased to 0. 8w for simulation, and the curve is shown in Fig. 7. The output power can reach 6. 98×10^{-9}w, which is about 40% higher than 0. 6w pump power, and the pump power is the key factor affecting the output spectrum.

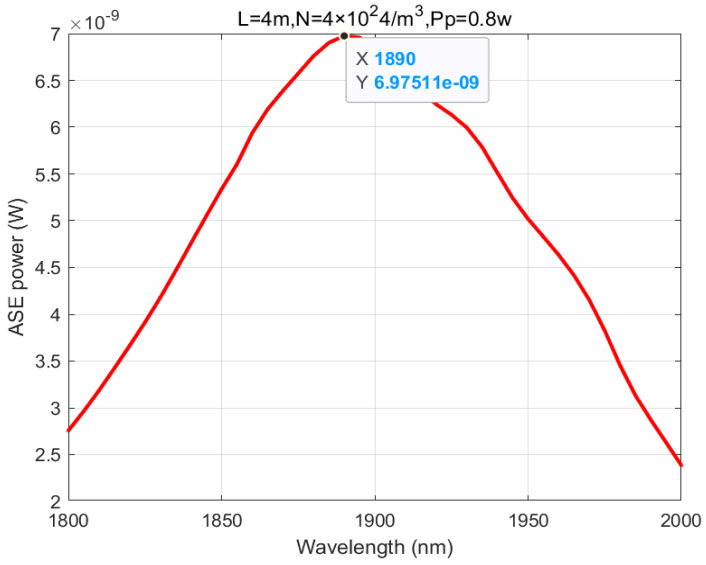

Fig 7. Output spectrum at pump power of 0. 8w.

Benefiting from the current technological advances, Thulium-doped optical fiber has made significant achievements in recent years. The wavelength of the fiber currently in use is in the range of 1500nm. By studying the output spectrum in the range of 1400-1520nm versus 1800-2000nm, it

can be found that there is a significant change in the output spectrum of the latter range. Therefore, further studies can be conducted in the band around 2000 nm.

Thulium-doped optical fibers are still used in many fields, for example, in the medical field to cut cells more precisely and in the industry to analyze the absorption spectrum of carbon dioxide in the air to determine the composition of the air quickly. Thulium-doped optical fiber is undoubtedly the focus of future research. The increase in fiber optic transmission speed will bring rapid development to society, and the development of fiber optic transmission prospects will be very broad.

4. Conclusion

Changing the length of Thulium-doped light, doping concentration, and pump power, between the three, and the pump power has the greatest effect on the output power of the fiber. Meanwhile, the output spectrum of Thulium-doped fiber is mainly concentrated in the 1800-2000nm band, and the output power of about 4. 98×10^{-9}w can be obtained at L=4m, doping concentration N=2×10^{24}, and pump power 0. 6w. meanwhile, if the pump power is increased with a constant length and doping concentration, the output power will continue to increase. However, the pump power cannot be increased indefinitely due to the limitation of conditions.

References

[1] Jin Xiaoxi. Research on high power Thulium-doped fiber laser power calibration and amplification [D]. University of Defense Science and Technology, 2015.

[2] Feng Gaofeng, Zhang Haifeng, Ge Xiliang. Development of high efficiency double-clad Thulium-doped optical fiber [J]. Modern Transmission, 2015(06):72-74.

[3] Zhu Shanying, Cao Huimin, Xie Qinlan, Zheng Dongyun. Research on optical fiber moisture sensor based on spectral absorption [J]. Sensors and Microsystems, 2012, 31(10):31-33+37. .

[4] Yang Xiangdi, Chen Yue, Li Dan, Wang Haoyu, Zhang Jianglin. Application and research progress of semiconductor laser in dental clinical care [J]. Journal of Laser Biology, 2015, 24(03):226-231.

[5] Yi, H. Y., Qi, Y., Huang, J. J. Progress in the development of shipborne laser weapons [J]. Laser Technology, 2015, 39(06):834-839.

[6] Zhang L, Sun YN, Wang WJ, Li TJ. Progress of research and application of femtosecond laser in industry [J]. Thermal Processing Technology, 2020, 49(10):20-24.

[7] Yang R, Dong JH, Yang ZH, Chen C, Li XF, Zhou DF, Shi YL. Advances in bioaerosol laser remote detection technology [J/OL]. Laser Journal:1-10, 2022

[8] Lin Y, Liu MQ, Ouyang DQ, Xiao KF, Chen YW, Lv QT, Ruan SSC. Experimental investigation of extracorporeal lithotripsy based on Thulium-doped fiber laser [J]. China Laser, 2022, 49(01):179-187.

[9] Li X, Yang Chao, Li YL. Research progress of 2μm high power Thulium-doped continuous fiber laser [J]. Laser Journal, 2022, 43(11):1-5.

[10] Wang Xiao-Fa, Zhang Jun-Hong, Gao Zi-Ye, Xia Guang-Qiong, Wu Zheng-Mao. Nanosecond mode-locked Thulium-doped fiber laser based on graphene saturable absorber [J]. Journal of Physics, 2017, 66(11):172-177.

[11] Zhang Haiwei, Sheng Quan, Shi Wei, Bai Xiaolei, Fu Shijie, Yao Jianquan. Temperature distribution characteristics of high power double-clad Thulium-doped fiber amplifier (in English) [J]. Infrared and Laser Engineering, 2017, 46(06):200-207.

[12] Zhang W, Wu W D, Yu T, Meng J, Yang C, Chen X L, Liu C M, Ye X S. Research on high power narrow spectrum width 1915 nm Thulium-doped fiber laser[J]. Infrared and Laser Engineering, 2018, 47(05):73-79.

[13] Xunjie Wang, Cheng Wang, Yanni Yang, Yang-Yang Over. Study on the effect of new inner cladding shape on the absorption efficiency of Thulium-doped double-clad optical fiber [J]. Advances in Laser and Optoelectronics, 2021, 58(17):235-239.

[14] Mira Naftaly, Shaoxiong Shen, Animesh Jha, Tm3+-doped tellurite glass for a broadband amplifier at 1. 47 mm, 20 September 2000 y Vol. 39, No. 27 y APPLIED OPTICS

[15] Yuki Kishi and Setsuhisa Tanabe, Properties of Tm31-Doped Germanotellurite Glasses for S-Band Amplifier, J. Am. Ceram. Soc. 89 [1] 236–240 (2006).

[16] Yin-Wen Lee, Han-Wei Tseng, Che-Hung Cho, Ju-Zhe Chen, Juin-Shin Chang, Shibin Jiang, Heavily Tm3+-Doped Silicate Fiber for High-Gain Fiber Amplifiers, Fibers 2013, 1, 82-92; doi:10. 3390/fib1030082